British Journal of Pharmacology (2009), 156, 649–661

0007-1188/09
www.brjpharmacol.org

RESEARCH PAPER

Glutamate-induced post-activation inhibition of locus coeruleus neurons is mediated by AMPA/kainate receptors and sodium-dependent potassium currents

Teresa Zamalloa[1], Christopher P. Bailey[2] and Joseba Pineda[1]

[1]*Department of Pharmacology, Faculty of Medicine, University of the Basque Country, Bizkaia, Spain, and* [2]*Department of Pharmacology, School of Medical Sciences, University of Bristol, Bristol, UK*

Background and purpose: Locus coeruleus (LC) neurons respond to sensory stimuli with a glutamate-triggered burst of spikes followed by an inhibition. The aim of our work was to characterize the inhibitory effect of glutamate in the LC.
Experimental approach: Single-unit extracellular and patch-clamp recordings were performed to examine glutamate responses in rat brain slices containing the LC.
Key results: Glutamate caused an initial activation followed by a late post-activation inhibition (PAI). Both effects were blocked by an AMPA/kainate receptor antagonist but not by NMDA or metabotropic glutamate receptor antagonists. All glutamate receptor agonists were able to activate neurons, but only AMPA and quisqualate caused inhibition. In neurons clamped at −60 mV, glutamate and AMPA induced inward, followed by outward, currents, with the latter reversing polarity at −110 mV. Glutamate-induced PAI was not modified by α_2-adrenoceptor, μ opioid, A_1 adenosine and $GABA_{A/B}$ receptor antagonists or Ca^{2+}-dependent release blockade, but it was reduced by raising the extracellular K^+ concentration. Glutamate-induced PAI was not affected by several potassium channel, Na^+/K^+ pump, PKC and neuronal NO synthase inhibitors or lowering the extracellular Ca^{2+} concentration. The Na^+-activated K channel opener bithionol concentration-dependently potentiated glutamate-induced PAI, whereas partial (80%) Na^+ replacement reduced glutamate- and AMPA-induced PAI. Finally, reverse transcription polymerase chain reaction assays showed the presence of mRNA for the Ca^{2+}-impermeable GluR2 subunit in the LC.
Conclusions and implications: Glutamate induces a late PAI in the LC, which may be mediated by a novel postsynaptic Na^+-dependent K^+ current triggered by AMPA/kainate receptors.
British Journal of Pharmacology (2009) **156,** 649–661; doi:10.1111/j.1476-5381.2008.00004.x

Keywords: glutamate; AMPA; post-activation inhibition; locus coeruleus; K_{Na}; *in vitro* electrophysiology

Abbreviations: aCSF, artificial cerebrospinal fluid; CNQX, 6-cyano-7-nitroquinoxaline-2,3-dione; CPDPX, 8-cyclopentyl-1,3-dipropylxanthine; D-AP5, D-(-)-2-amino-5-phosphonopentanoic acid; iGluR, ionotropic glutamate receptor; K_{Na}, Na^+-activated K channels; LC, locus coeruleus; mGluR, metabotropic glutamate receptor; PAI, post-activation inhibition; RSMCPG, RS-methyl-4-carboxyphenylglycine; tACPD, trans-(±)-1-amino-1,3-cyclopentanedicarboxylic acid; TEA, tetraethylammonium chloride

Introduction

The locus coeruleus (LC) is the main noradrenergic nucleus in the brain (Dahlstrom and Fuxe, 1965). The compact and homogeneous nature of this nucleus in the rat has long allowed the study of the physiology of central noradrenergic neurons *in vitro* and *in vivo* (Svensson *et al.*, 1975; Aghajanian *et al.*, 1983). The LC participates in brain functions such as vigilance, attention, learning or memory (Aston-Jones and Cohen, 2005) and psychiatric disorders such as anxiety, depression or stress (Berridge and Waterhouse, 2003). It has been used as a model for examining drug actions in the brain (Nestler and Aghajanian, 1997; Chao and Nestler, 2004). Previous studies *in vivo* have shown that LC neurons maintain a spontaneous tonic discharging activity, which is regulated by a wide variety of sensory stimuli (see Aston-Jones and Cohen, 2005). Simple and conditioned external stimuli activate LC cells in conscious animals, whereas painful and visceral stimuli activate LC cells in anaesthetized rats. Activation of LC cells by noxious and non-noxious physiological sensory stimuli is typically characterized by a brief interval of burst firing followed by a long-lasting period of inhibited activity [(post-activation inhibition (PAI)]

Correspondence: Dr Joseba Pineda, Department of Pharmacology, Faculty of Medicine, University of the Basque Country. Barrio Sarriena s/n, E-48940 Leioa, Bizkaia, Spain. E-mail: joseba.pineda@ehu.es
Received 12 May 2008; revised 12 August 2008; accepted 16 August 2008

(Cedarbaum and Aghajanian, 1976; Foote *et al*., 1980). The precise mechanism responsible for this PAI is unclear. Two theories have emerged on the basis of antidromic, orthodromic and intracellular stimuli assays: (i) depolarization-evoked release of noradrenaline from intracoerulear recurrent collaterals or dendrites, which inhibits LC cells through α_2-adrenoceptors (Aghajanian *et al*., 1977; Cedarbaum and Aghajanian, 1978; Aghajanian and VanderMaelen, 1982; Ennis and Aston-Jones, 1986); and (ii) intrinsic spike-induced, Ca^{2+}-activated K^+ currents in the somatodendritic membrane, which prolong the after-hyperpolarization of LC neurons (Andrade and Aghajanian, 1984). In either case, glutamate release in the LC seems to be the trigger of the activation-inhibition response (Ennis and Aston-Jones, 1988). This excitatory neurotransmitter is released by projections arising from the paragigantocellularis nucleus in the medulla (Chiang and Aston-Jones, 1993).

The involvement of glutamatergic transmission in the PAI has been established by indirect procedures, consisting of electrical stimuli of the hind paw, electrical lesions of the paragigantocellularis nucleus and combined administrations of glutamate receptor antagonists. Direct support for a functional role of glutamate and glutamate receptors in the LC has been attained only for the activatory effect but not for the inhibition (Masuko *et al*., 1986; Olpe *et al*., 1989). Thus, LC neurons from slice preparations are activated by agonists for all classes of ionotropic glutamate receptors (iGluR; by glutamate, NMDA, AMPA, kainate or quisqualate) and, to a lesser extent, for metabotropic glutamate receptors [mGluR; by trans-(±)-1-amino-1,3-cyclopentanedicarboxylic acid (tACPD)] (Masuko *et al*., 1986; Olpe *et al*., 1989). Therefore, the aim of the present work was to characterize, by electrophysiological techniques, the effects of glutamate on LC neurons from rat brain slices, with especial focus on the PAI, and to characterize the receptor subtypes and possible mechanisms that are involved in these effects.

Methods

Test systems used

Brain slice preparation. All animal procedures were carried out in accordance with the European Community Council Directive on 'Protection of Animals Used in Experimental and Other Scientific Purposes' of 24 November 1986 (86/609/EEC). Every effort was made to minimize animal suffering and to use the minimum possible number of animals. Animals were housed under standard laboratory conditions (22°C, 12 h light/dark cycles, food and water *ad libitum*). Experiments were performed in 150 male Sprague-Dawley (200–300 g) or 16 Wistar (130–170 g) rats.

When extracellular recordings were to be carried out, Sprague-Dawley rats were first anaesthetized with chloral hydrate (400 mg·kg^{-1}, i.p.) and decapitated. The brain was extracted and a block of tissue containing the brainstem was rapidly immersed in ice-cold artificial cerebrospinal fluid (aCSF) containing (in mmol·L^{-1}): NaCl 126, KCl 3, NaH_2PO_4 1.25, glucose 10, $NaHCO_3$ 25, $CaCl_2$ 2 and $MgSO_4$ 2. Coronal slices of 500 μm thickness containing the LC were cut using a vibratome, placed in a nylon mesh and incubated at 33 ± 0.5°C in a modified Haas-type interface chamber which provided excellent perfusion to the slice. The tissue was continuously perfused with aCSF saturated with 95% O_2/5% CO_2 (for a final pH of ~7.34), at a flow rate of 1.5 mL·min^{-1}, and left to equilibrate for at least 1 h before recordings were made. When the concentration of KCl was modified for the experiment, the composition of NaCl was also adjusted for equi-osmolarity.

When whole-cell patch-clamp recordings were to be made, Wistar rats were decapitated, and the brains were extracted and rapidly submerged in ice-cold cutting solution containing the following composition (in mmol·L^{-1}): NaCl 20, KCl 2.5, $CaCl_2$ 0.5, $MgCl_2$ 7, NaH_2PO_4 1.25, sucrose 85, D-glucose 25 and $NaHCO_3$ 60. Coronal slices of 250 μm thickness containing the LC were prepared using a vibratome. Immediately after cutting, slices were submerged in aCSF containing (in mmol·L^{-1}): NaCl 126, KCl 2.5, $MgCl_2$ 1.2, $CaCl_2$ 2.4, NaH_2PO_4 1.2, D-glucose 11.1, $NaHCO_3$ 21.4 and ascorbic acid 0.1 (saturated with 95% O_2/5% CO_2 at 34°C). Slices were submerged in a slice chamber (0.5 mL) and perfused with aCSF at a flow rate of 2.5–3 mL·min^{-1} at 33–34°C. The slice was left to equilibrate for at least 1 h before recordings were made.

Measurements

Extracellular recordings. Single-unit extracellular recordings of LC cells were made as previously described (Pineda *et al*., 1996). The recording electrode, which consisted of an Omega-dot glass micropipette, was pulled and filled with NaCl (0.05 mol·L^{-1}). The tip was broken back to a diameter of 2–5 μm (3–5 MΩ). The electrode was positioned in the LC, which was identified visually in the rostral pons as a dark oval area on the lateral borders of the central gray and the 4th ventricle, just anterior to the genu of the facial nerve. The extracellular signal from the electrode was passed through a high-input impedance amplifier and monitored on an oscilloscope and also with an audio unit. Individual neuronal spikes were isolated from the background noise with a window discriminator and the firing rate was analysed by means of a PC-based custom-made programme, which generated histogram bars representing the cumulative number of spikes in consecutive 10 s bins (HFCP®, Cibertec S.A., Madrid, Spain). Noradrenergic cells were identified by their spontaneous and regular discharge activity, the slow firing rate and the long-lasting, positive-negative waveforms (Andrade and Aghajanian, 1984).

Patch-clamp recordings. Whole-cell patch-clamp recordings were performed as described previously by Bailey *et al*. (2003). LC neurons were visualized by Nomarski optics, and individual cell somata were cleaned by gentle flow of aCSF from a pipette. Whole-cell voltage-clamp recordings (V_h of –60 mV) were made using electrodes (3–6 MΩ) filled with the following solution (in mmol·L^{-1}): K gluconate 115, HEPES 10, EGTA 11, $MgCl_2$ 2, NaCl 10, MgATP 2 and Na_2GTP 0.25 (pH of 7.3) (270 mOsm). Recordings were filtered at 2 kHz using an Axopatch 200B amplifier (Axon Instruments, Foster City, CA, USA) and displayed on a chart recorder (Gould Instruments, Loughton, UK). The resting membrane potential was kept at –60 mV and, to study the ionic mechanism underlying the outward current caused by glutamate, voltage ramps from

–140 to –60 mV were imposed. This protocol provides direct records of the voltage-current relationship with the voltage as abscissa and the current as ordinate.

Reverse transcription polymerase chain reaction. Total RNA was isolated from the cerebral cortex and the LC of male Wistar rats (150 g) by a TriZol reagent (Invitrogen). Single-strand cDNA was transcribed using M-MLV reverse transcriptase (Promega) and random hexanucleotide primers (Roche). cDNAs were amplified by Biotaq polymerase (Bioline) and primers as indicated below. To make sure that cDNA synthesis was correct, glycerol-3-phosphate dehydrogenase (GAPDH) was used as an internal control. Sequences of the primers were: GAPDH forward: 5′-CCACCCATGGCAAATTCCATG GCA-3′; GAPDH reverse: 5′-TCTAGACGGCAGGTCAGG TCCACC-3′; GluR1 forward: 5′-ATGCCGTACATCTTTGCC-3′; GluR1 reverse: 5′-AACAGGAAAACTTGGAGTA-3′; GluR2 forward: 5′-GCCAACAGTTTCGCAGTC-3′; GluR2 reverse: 5′-TTTATCCCTTTCACAGTCCAG-3′. Generally, annealing was performed at 55°C for 1 min, and extension at 72°C for 30 s. The resulting products were subjected to electrophoresis on a 1.5% agarose gel containing ethidium bromide (0.8 $\mu g \cdot mL^{-1}$) and photographed under UV illumination. Band density was quantified using Kodak ID3.6 software.

Experimental design
The firing rate of LC neurons was recorded for several minutes before the drug application to ensure stability and obtain the baseline activity. To characterize the effects mediated by glutamate receptors, we recorded the firing rate of LC neurons before (baseline), during and after perfusion with glutamate, NMDA, AMPA, kainate, tACPD or quisqualate, in accordance with previous results in the LC (Olpe *et al*., 1989; Kogan and Aghajanian, 1995; Dubé and Marshall, 1997). The effect of glutamate was also measured before and after the glutamate receptor antagonists D-(-)-2-Amino-5-phosphonopentanoic acid (D-AP5), 6-cyano-7-nitroquinoxaline-2,3-dione disodium salt (CNQX) or RS-methyl-4-carboxyphenylglycine (RS-MCPG), on the basis of previous data in the LC (Olpe *et al*., 1989; Kogan and Aghajanian, 1995; Dubé and Marshall, 1997). To unmask the presynaptic/postsynaptic nature of glutamate-induced PAI, we assessed the following antagonists for inhibitory receptors: naloxone (for μ opioid receptors), RS79948 or idazoxan (for α_2-adrenoceptors), 8-cyclopentyl-1,3-dipropylxanthine (CPDPX) (for A_1 adenosine receptors), picrotoxin (for $GABA_A$ receptors) and phaclofen (for $GABA_B$ receptors), at the same concentrations used by other authors in the LC (Pepper and Henderson, 1980; Olpe *et al*., 1988; Regenold and Illes, 1990; Fernández-Pastor and Meana, 2002). To characterize the ionic mechanisms involved in the inhibitory effect of glutamate, we used the following K^+ current blockers: tetraethylammonium (TEA; broad spectrum for K channels), Ba^{2+} (for inward-rectifier K channels), apamine and charybdotoxin (for Ca^{2+}-activated K channels) or ouabain (for Na^+/K^+ pump). To further explore the involvement of Na^+-activated K channels (K_{Na}), we evaluated the effect of the K_{Na} opener bithionol and a partial replacement (60% and 80%) of Na^+ by choline-HCl in the presence of atropine (5 $\mu mol \cdot L^{-1}$) (to block muscarinic responses). In all the experiments, the inhibitor/blocker was perfused for at least 10 min and the reproducibility of glutamate effects was confirmed several times before the drug application.

Data analysis and statistical procedures
The firing rates before and after the different experimental manipulations were obtained from the recorded 10 s bin rate histograms and, in certain cases, expressed as the percentages of the baseline firing rates. The *baseline* value was the average firing rate obtained from three consecutive bins prior to each application. The firing rate corresponding to the *initial* activation period was obtained during the peak effect (i.e. the bin with the highest discharging rate after the onset of agonist application). The rate value corresponding to the *late* post-activation period was the average firing rate of 5–8 consecutive bins obtained within 2 min of the peak, and subsequently every 30 s (the number of bins counted to obtain the *late* rate value was always the same within each cell and group). The activatory effect of agonists was calculated by subtracting the baseline firing rate from the rate during the initial activation, whereas the inhibitory effect was estimated by subtracting the firing rates during the late post-activation from the baseline rate; when needed, these effects were expressed as percentages of the initial firing rate. To facilitate comparisons of glutamate responses under different experimental situations, we calculated in each cell the ratio of glutamate response after the experimental manipulation with respect to the basal glutamate response (i.e. the post-manipulation glutamate effect divided by the pre-manipulation glutamate effect). Whenever a significant change in the spontaneous firing rate was encountered after drug application or manipulation, the glutamate responses were normalized with respect to a test concentration of GABA.

To evaluate concentration-effect curves, fitting analysis was performed by the computer programme GraphPad Prism (version 3.0 for Windows, San Diego, CA, USA) to obtain the best simple nonlinear fit to the following three-parameter logistic equation: $E = E_{max}/[1 + (EC_{50}/A)^n]$, where E is the effect induced by each concentration of the agonist (A), E_{max} is the maximal effect, EC_{50} is the concentration of the agonist needed to elicit a 50% of the maximal effect and n is the slope factor of the concentration-effect curve. These parameters were determined in individual assays by the nonlinear analysis and then averaged to obtain the theoretical parameters in each group.

Data are expressed as mean ± SEM. The *n* values represent the number of slices. Statistical significances were evaluated by the paired Student's *t*-test (when the firing rates or response data were compared before and after test applications within cells) or by the two-sample Student's *t*-test (when the firing rates or response values were compared under two independent experimental situations). One-way analysis of variance (ANOVA) followed by the *post hoc* Tukey's *t*-test was used when firing rates or response values were compared under more than two experimental situations. A two-tailed probability level of 0.05 was accepted as significantly different.

Drugs
The following drugs were purchased from Sigma-Aldrich Química S.A. (Madrid, Spain): *trans*-(±)-1-amino-1,3-

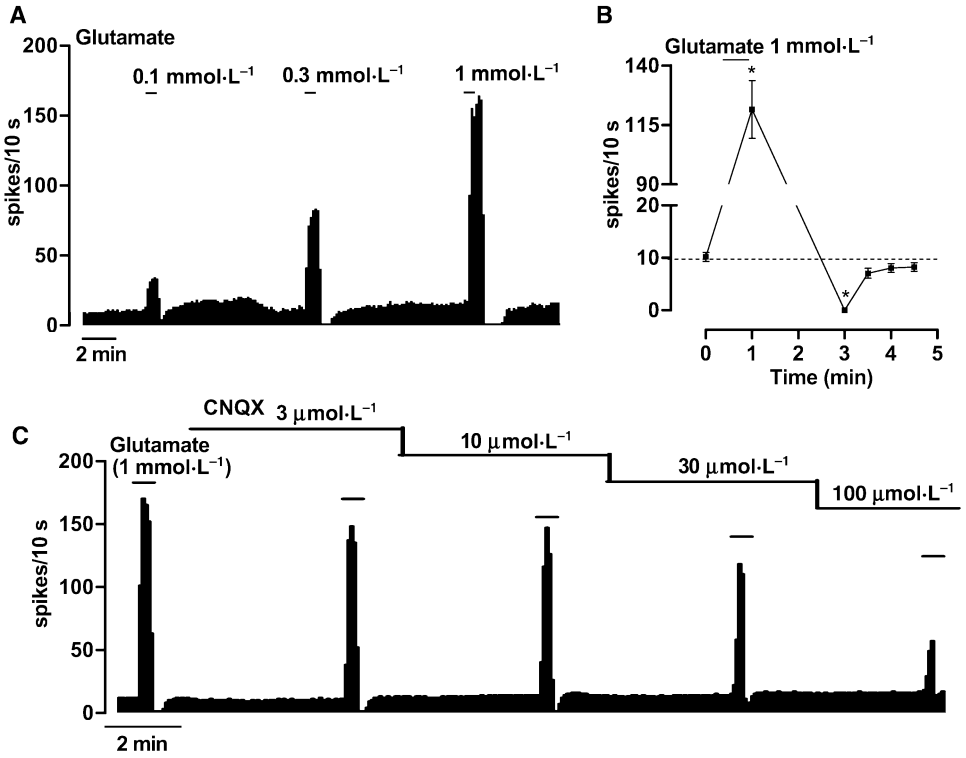

Figure 1 Effect of glutamate on the firing activity of LC neurons. A. Representative example of the firing rate recording of a neuron showing the concentration-dependent activation and PAI induced by glutamate (0.1–1 mmol·L^{-1}). The vertical lines represent the integrated firing rate (spikes per 10 s). Glutamate was applied to yield the bath concentration shown and for the time indicated by the horizontal bars. B. Time course of the firing rate of LC neurons before (time = 0) and after administration of glutamate (during *initial* activation and *late* post-activation periods; see *Methods*). Symbols represent mean ± SEM of 17 experiments. *P < 0.005 compared with the basal firing rate by a paired Student's *t*-test. C. Representative example of the firing rate recording of a neuron showing the effect of glutamate (1 mmol·L^{-1}) before and after 10 min applications of increasing concentrations of CNQX (3–100 μmol·L^{-1}).

cyclopentanedicarboxylic acid (tACPD), AMPA, apamine, atropine, Ba^{2+}, bithionol, Cd^{2+}, chloral hydrate, charybdotoxin, CPDPX, GABA, L-glutamic acid, idazoxan, kainic acid, NMDA, naloxone, 7-nitroindazole, ouabain, picrotoxin, (+)-quisqualic acid, RS-MCPG and tetraethylammonium chloride (TEA). D-AP5, chelerythrine chloride, CNQX, phaclofen (racemic) and RS79948 hydrochloride were obtained from Tocris Cookson Ltd. (UK). All drugs were dissolved in water as stock solutions, stored at –25°C and then diluted in aCSF just before each experiment for bath application. Drugs were applied in the perfusing solution. Antagonists, blockers and other experimental manipulations were applied for at least 10 min before testing their influence on glutamate effects. The receptor and ion channel nomenclature used in the present document conforms to the BJP's Guide to Receptors and Channels (Alexander *et al.*, 2008).

Results

Effect of glutamate on the firing rate of LC neurons

Perfusion with glutamate (0.03–3 mmol·L^{-1}, 30 s) caused a concentration-dependent increase in the firing rate of LC neurons (E_{max} = 17.5 ± 3.5 Hz, EC_{50} = 595 ± 124 μmol·L^{-1}, n = 6) (Figures 1A and 4A). This activation was followed by a late PAI (Figures 1A and 4B), which was also dependent on the concentration of glutamate (0.03–1 mmol·L^{-1}; EC_{50} = 392 ± 101 μmol·L^{-1}). To better examine the time course of the biphasic response of LC neurons to glutamate, a submaximal concentration (1 mmol·L^{-1}) of this drug was used in subsequent experiments. In all cells tested (n = 21), perfusion with glutamate (1 mmol·L^{-1}, 30 s) induced a 10- to 15-fold increase (P < 0.001) in the firing rate of LC neurons, which peaked within 1 min of the application. After the early activation, 17 out of these 21 cells stopped firing for an interval of 30–45 s (Figure 1A,B). When glutamate was subsequently washed out, the normal spontaneous firing activity resumed within 2–3 min (Figure 1A,B).

To characterize the receptor subtype involved in the post-activation inhibitory effect of glutamate, we examined glutamate effects before and after glutamate receptor antagonists. No significant modification of activation or PAI induced by glutamate was observed after application of the selective NMDA receptor antagonist D-AP5 (200 μmol·L^{-1}) (n = 4) (Table 1) or the non-selective mGluR antagonist RS-MCPG (0.5 mmol·L^{-1}) (n = 2; data not shown), indicating that NMDA or metabotropic glutamate receptors were not the main factors involved in these responses. However, perfusion with the AMPA/kainate receptor antagonist CNQX (3–100 μmol·L^{-1}) concentration-dependently reduced both the activation (n = 5, P < 0.05) and the PAI (n = 5, P < 0.05) induced by glutamate (Figure 1C and Table 1). CNQX concentrations required to block glutamate-induced activation (30 μmol·L^{-1}) were lower than those needed to block PAI (100 μmol·L^{-1}).

Table 1 Effect of glutamate receptor antagonists and manipulations of presynaptic and ionic mechanisms on glutamate-induced early activation and post-activation inhibition in LC neurons from brain slices

Experimental manipulations	*Early activation*			*Post-activation inhibition*			
	Ratio[a]	*Predrug*[b] *(spikes/10 s)*	*Postdrug*[b] *(spikes/10 s)*	*Ratio*[a]	*Predrug*[c] *(spikes/10 s)*	*Postdrug*[c] *(spikes/10 s)*	n
Antagonists							
D-AP5 0.2 mmol·L^{-1}	0.92 ± 0.00	79 ± 19	81 ± 18	1.45 ± 0.21	10 ± 3	13 ± 7	4
CNQX 3 μmol·L^{-1}	0.92 ± 0.03*	155 ± 18	142 ± 17	0.94 ± 0.08	13 ± 1	12 ± 2	5
10 μmol·L^{-1}	0.81 ± 0.08*	182 ± 31	154 ± 35	1.10 ± 0.18	13 ± 2	14 ± 3	5
30 μmol·L^{-1}	0.68 ± 0.13*	182 ± 31	134 ± 39	0.94 ± 0.18	13 ± 2	11 ± 3	5
100 μmol·L^{-1}	0.35 ± 0.11**	150 ± 27	79 ± 25	0.39 ± 0.17*	14 ± 2	5 ± 3	5
Presynaptic mechanism							
Naloxone 10 μmol·L^{-1}	0.95 ± 0.07	116 ± 33	102 ± 24	0.99 ± 0.03	10 ± 3	10 ± 3	5
RS79948 1 μmol·L^{-1}	0.97 ± 0.05	115 ± 20	111 ± 18	1.08 ± 0.19	7 ± 1	7 ± 1	5
Idazoxan 10 μmol·L^{-1}	1.04 ± 0.09	79 ± 24	84 ± 16	1.07 ± 0.08	8 ± 0	10 ± 3	5
CPDPX 0.1 μmol·L^{-1}	0.91 ± 0.10	127 ± 35	109 ± 26	0.78 ± 0.10	11 ± 2	8 ± 2	6
Picrotoxin 0.1 mmol·L^{-1}	0.98 ± 0.10	100 ± 15	101 ± 24	0.90 ± 0.06	7 ± 1	7 ± 1	5
Phaclofen 0.3 mmol·L^{-1}	1.03 ± 0.03	111 ± 13	115 ± 15	1.16 ± 0.17	10 ± 1	11 ± 3	4
Cadmium 50 μmol·L^{-1}	2.76 ± 0.50*	103 ± 7	288 ± 60	1.26 ± 0.14	7 ± 2	8 ± 1	5
Ionic mechanism							
KCl 18 mmol·L^{-1}	0.45 ± 0.067**	129 ± 8	57 ± 9	0.57 ± 0.11*	13 ± 2	7 ± 1	5
TEA 10 mmol·L^{-1}	0.54 ± 0.05*	117 ± 23	61 ± 9	1.03 ± 0.03	10 ± 1	10 ± 1	5
Apamine 0.2 μmol·L^{-1}	1.81 ± 0.24*	87 ± 6	159 ± 25	0.99 ± 0.12	9 ± 2	9 ± 2	5
Charyb 40 nmol·L^{-1}	0.97 ± 0.06	127 ± 35	127 ± 40	1.04 ± 0.01	11 ± 1	11 ± 1	3
150 nmol·L^{-1}	0.72 ± 0.23	148 ± 46	126 ± 55	0.93 ± 0.26	11 ± 3	8 ± 1	3
Barium 0.3 mmol·L^{-1}	0.95 ± 0.18	110 ± 17	93 ± 9	0.73 ± 0.14	11 ± 2	7 ± 1	5
Ouabain 0.5 μmol·L^{-1}	1.04 ± 0.08	108 ± 12	111 ± 11	1.06 ± 0.09	10 ± 2	12 ± 3	5
Ca^{2+} 0.2 mmol·L^{-1}	1.45 ± 0.29	119 ± 20	160 ± 27	0.70 ± 0.12	9 ± 1	6 ± 2	6
Bithionol 10 μmol·L^{-1}	0.76 ± 0.29	74 ± 23	43 ± 12	2.47 ± 0.57*	2 ± 0	6 ± 1	3
Na^{+} substitution							
60%	0.67 ± 0.11	127 ± 15	81 ± 16	0.95 ± 0.13	15 ± 3	14 ± 4	7
80%	0.38 ± 0.08**	123 ± 18	48 ± 10	0.33 ± 0.16**	12 ± 1	4 ± 2	6

Data represent the means ± SEM. *$P < 0.05$, **$P < 0.01$ when postdrug values were compared with predrug values (paired Student's *t*-test).
[a]The ratio was estimated in each cell as the postdrug glutamate effect divided by the predrug glutamate effect.
[b]The predrug and postdrug activation values were calculated in each cell as the increments in the firing rate induced by glutamate from the baseline rate, before and after the experimental manipulation.
[c]The predrug and postdrug post-activation inhibition values were calculated in each cell as the reductions in the firing rate induced by glutamate from the baseline rate, before and after the experimental manipulation.
Charyb, charybdotoxin.

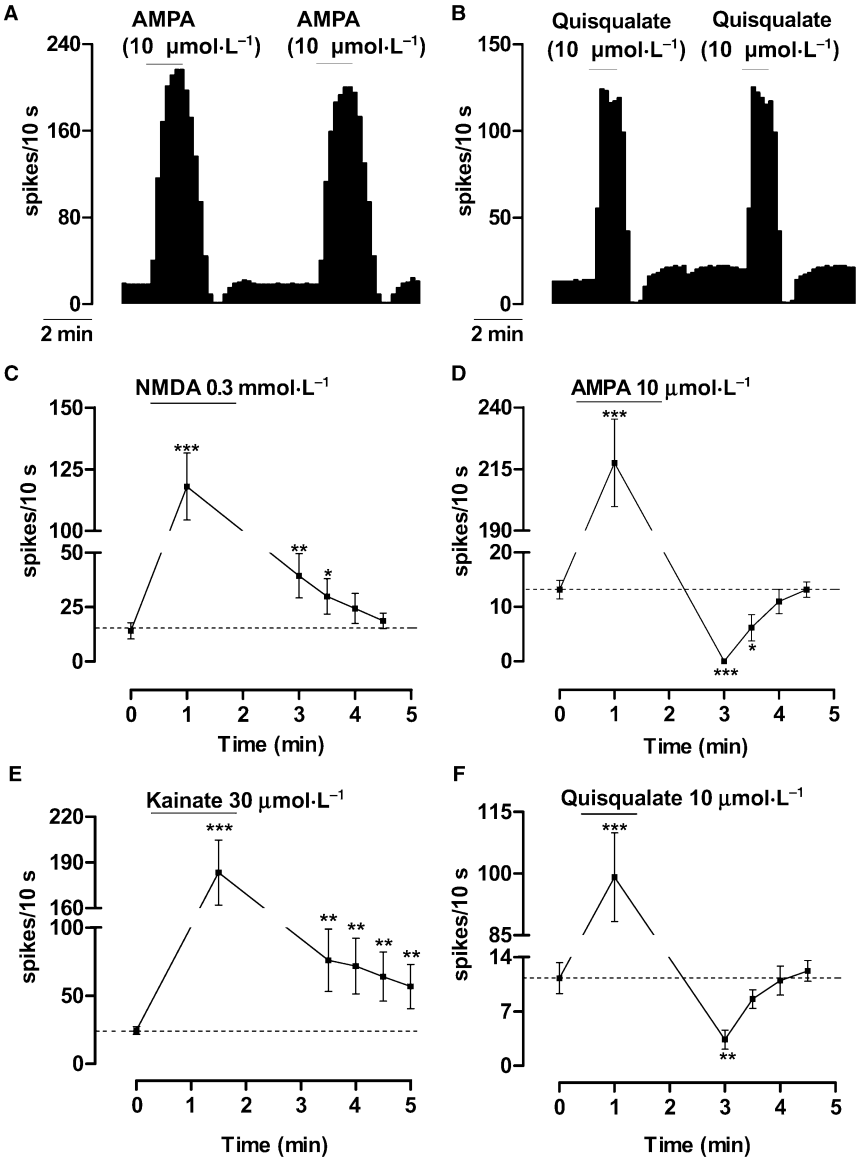

Figure 2 Effect of iGluR agonists on the firing rate of LC neurons. A, B. Representative examples of firing-rate recording which show the effect of AMPA (10 µmol·L^{-1}, 90 s) (A) and quisqualate (10 µmol·L^{-1}, 60 s) (B) on the firing rate of LC neurons. Each vertical line represents the integrated firing rate (spikes per 10 s). Drugs were applied to yield the bath concentration shown and for the time indicated by the horizontal bars. C–F. Time course of the firing rate of LC neurons before (time = 0) and after perfusion with NMDA (0.3 µmol·L^{-1}) ($n = 9$) (C), AMPA (10 µmol·L^{-1}) ($n = 11$) (D), kainate (30 µmol·L^{-1}) ($n = 7$) (E) and quisqualate (10 µmol·L^{-1}) ($n = 7$) (F). Symbols represent mean ± SEM of n experiments. *$P < 0.05$, **$P < 0.01$, ***$P < 0.005$ compared with the basal firing rate by a paired Student's t-test.

Effect of glutamate receptor subtype agonists on the firing rate of LC neurons

In order to further characterize which receptor subtype is involved in the effects of glutamate, we applied various agonists of iGluR and mGluR. As expected, single concentrations of agonists for iGluR (NMDA 300 µmol·L^{-1}, AMPA 10 µmol·L^{-1}, kainate 30 µmol·L^{-1}) or mGluR (tACPD 100 µmol·L^{-1}) caused strong activations of LC neurons ($n = 9$, $P < 0.001$; $n = 11$, $P < 0.01$; $n = 7$, $P < 0.001$; $n = 11$, $P < 0.001$; respectively) (Figures 2A, C–E and 4A). Likewise, the mixed agonist of iGluR and mGluR quisqualate (10 µmol·L^{-1}, $n = 7$, $P < 0.001$) increased the firing rate of LC cells (Figure 2B,F). In these assays, AMPA and quisqualate were also able to induce a marked PAI (2A–B, D, F and 4B), whereas NMDA, kainate and tACPD failed to induce any inhibition following the activation of LC neurons (Figures 2C, E and 3A). Combinations of iGluR and mGluR agonists (NMDA 300 µmol·L^{-1} + tACPD 100 µmol·L^{-1}, $n = 3$; kainate 30 µmol·L^{-1} + tACPD 100 µmol·L^{-1}, $n = 5$) did not cause PAI (Figure 3B,C). To further confirm the different pharmacological profile of activatory and inhibitory effects, we performed concentration-effect curves for the iGluR agonists NMDA (10–300 µmol·L^{-1}), AMPA (0.3–10 µmol·L^{-1}) and kainate (1–30 µmol·L^{-1}) (Figure 4). For the activatory effect, we found the following rank order of potencies: AMPA ($EC_{50} = 3.9 \pm 1.0$ µmol·L^{-1}) > kainate ($EC_{50} = 19.0 \pm$

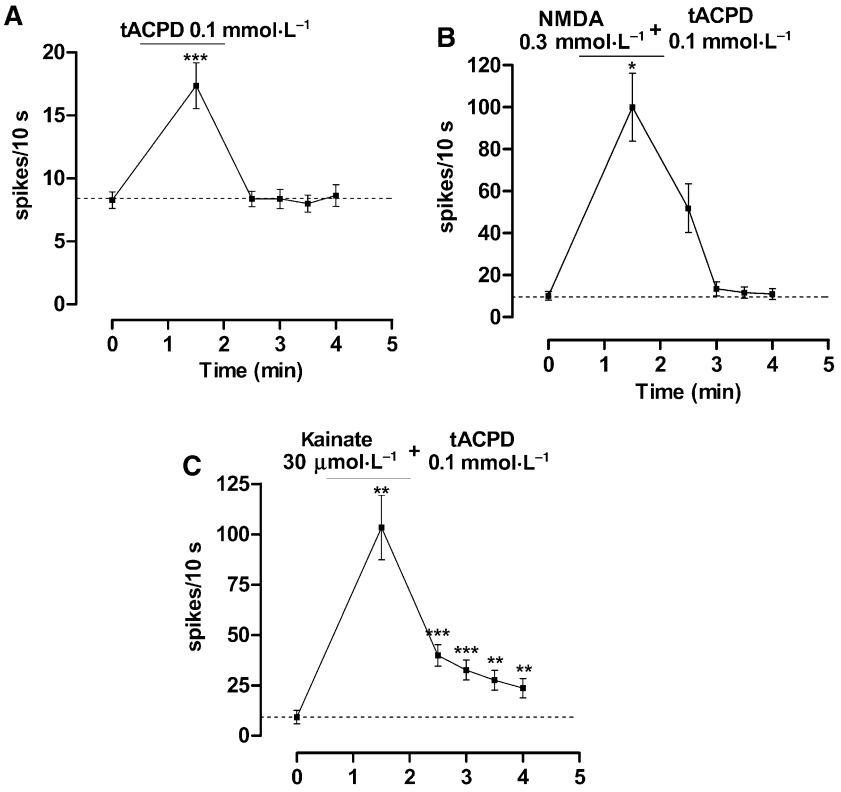

Figure 3 Time course of the firing rate of LC neurons before (time = 0) and after perfusion with tACPD (0.1 mmol·L^{-1}) (n = 11) (A), NMDA (0.3 mmol·L^{-1}) + tACPD (0.1 mmol·L^{-1}) (n = 3) (B) and kainate (10 µmol·L^{-1}) + tACPD (0.1 mmol·L^{-1}) (n = 5) (C). Symbols represent mean ± SEM of n experiments. *P < 0.05, **P < 0.01, ***P < 0.005 compared with the basal firing rate by a paired Student's t-test.

1.6 µmol·L^{-1}) > NMDA (EC_{50} = 99.9 ± 23.4 µmol·L^{-1}), with E_{max} values being 21.1 ± 6.0 Hz (n = 7), 17.5 ± 5.6 Hz (n = 3) and 14.9 ± 1.9 Hz (n = 7) respectively (Figure 4A). Interestingly, NMDA and kainate failed to induce PAI at any of the concentrations tested, but AMPA was able to cause PAI at concentrations when early activation was also observed (n = 7) (Figure 4B). AMPA was 30 to 100-fold more potent than glutamate in inducing PAI, but the steepness of the response precluded any meaningful determination of an EC_{50} for this effect (Figure 4B). These results confirm that AMPA receptor stimulation may be involved in the post-activation inhibitory effect of glutamate. In some cells, cessation of the firing activity of LC cells during very high firing periods (rates > 22 Hz) was associated with spike inactivation, as previously described (Olpe *et al.*, 1989). When this non-specific depolarization inactivation occurred, the cell was not used for the subsequent analysis of PAI. In fact, it differed from the observation described in the present work in several aspects. First, the *spike inactivation* appeared during the maximal activation (at the peak) and was always preceded by a broadening and shortening of the spike, whereas the *PAI* appeared after the neuronal activation (i.e. during the recovery phase) and was preceded by a normal spike waveform. Second, *spike inactivation* occurred regardless of the glutamate receptor agonist used, provided that the firing rate was very fast, whereas the *PAI* involved specific glutamate receptor agonists (see above).

Involvement of synaptic mechanisms in the effects of glutamate on LC neurons

In an effort to investigate a possible presynaptic mechanism involved in glutamate-induced PAI, we explored the effect of glutamate before and after antagonizing various inhibitory receptors known in the LC, or after blocking the Ca^{2+}-dependent neurotransmitter release. Neither the activation nor the PAI induced by glutamate was modified in the presence of the selective inhibitory receptor antagonists, including naloxone (10 µmol·L^{-1}, n = 5) (for µ opioid receptors), RS79948 (1 µmol·L^{-1}, n = 5) and idazoxan (10 µmol·L^{-1}, n = 5) (for α_2-adrenoceptors), CPDPX (0.1 µmol·L^{-1}, n = 6) (for A_1 adenosine receptors), picrotoxin (100 µmol·L^{-1}, n = 5) (for $GABA_A$ receptors) or phaclofen (300 µmol·L^{-1}, n = 4) (for $GABA_B$ receptors) (Table 1). Likewise, perfusion with the Ca channel blocker Cd^{2+} (50 µmol·L^{-1}) enhanced glutamate-induced activation but failed to change glutamate-induced PAI (Table 1). Taken together, these results suggest that PAI does not seem to be mediated by presynaptic release of inhibitory neurotransmitters.

Involvement of postsynaptic ionic and cellular mechanisms in the effect of glutamate on LC neurons

Since postsynaptic inhibitory responses in the LC are often mediated by K^+ currents, we explored the involvement of K^+-dependent currents in this phenomenon. Reducing the driving force of K^+ currents by a sixfold increase of K^+ concen-

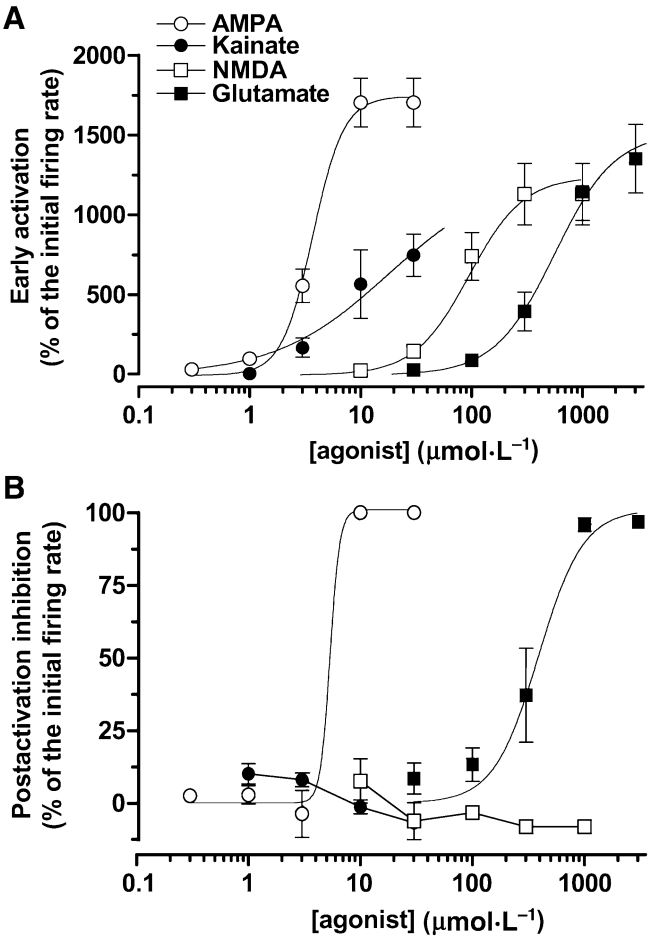

Figure 4 Dose-effect curves for glutamate receptor agonists showing the early activation (A) and the PAI (B) after perfusion with increasing concentrations of AMPA (0.3–10 μmol·L^{-1}), kainate (1–30 μmol·L^{-1}), NMDA (10–300 μmol·L^{-1}) and glutamate (30–1000 μmol·L^{-1}). Symbols represent mean ± SEM of *n* experiments (see below). Effect values were calculated as the increases or decreases of the firing rate from the baseline, after each drug application; these effect values were then normalized as percentages of the initial firing rates. The theoretical lines were obtained from the best nonlinear fitting of the three-parameter logistic equation to the individual curve data (see *Methods*). Note that the connecting lines are shown for the inhibitory curves of NMDA and kainate since they failed to induce PAI at any of the concentrations tested. EC_{50} and E_{max} values for these effects are described in the text (see *Results*).

trations in the aCSF (to 18 mmol·L^{-1}) attenuated, by 45%, the magnitude of the PAI induced by glutamate ($n = 5$, $P < 0.05$) (Table 1). This manipulation also reduced glutamate-induced activation of LC cells ($P < 0.01$) (Table 1). To confirm the involvement of a K^+ current by a direct measure of the membrane potential, whole-cell patch-clamping recordings were performed in LC neurons. In neurons clamped at –60 mV, application of glutamate (1 mmol·L^{-1}, 30 s) caused an inward followed by an outward current (98 ± 35 pA; $n = 11$) (Figure 5A). The outward current reversed polarity at –110 mV ($n = 4$), close to the predicted reversal potential of K^+ (–98 mV) under our experimental conditions (Figure 5C,E). Likewise, application of AMPA (3 μmol·L^{-1}, 90 s) induced a biphasic effect, with an inward followed by an outward current (Figure 5B) which reversed polarity at –102 mV (Figure 5D,F). These results confirm that the PAI induced by glutamate and AMPA may be mediated by a K^+-dependent mechanism.

Unexpectedly, hindering K^+ currents with the non-selective potassium channel blocker TEA (10 mmol·L^{-1}) only reduced the activation induced by glutamate ($n = 5$, $P < 0.05$), but it failed to modify the PAI ($n = 5$) (Table 1). Moreover, the PAI induced by glutamate was not modified by blocking specific K^+ currents such as small- and large-conductance Ca^{2+}-activated K channels (with apamine 0.2 μmol·L^{-1}, $n = 5$; and charybdotoxin 40 nmol·L^{-1}, $n = 3$ or 150 nmol·L^{-1}, $n = 3$; respectively), inward-rectifier K channels (with Ba^{2+} 0.3 mmol·L^{-1}, $n = 5$) or Na^+/K^+ pumping exchange (with ouabain 0.5 mmol·L^{-1}, $n = 5$) (Table 1). The involvement of a Ca^{2+}-dependent current (e.g. a Ca^{2+}-activated K channel) in the glutamate effect was further ruled out by perfusion with an aCSF containing low Ca^{2+} (0.2 mmol·L^{-1}), which failed to alter significantly the magnitude of glutamate-induced PAI (Table 1). Among the experimental manipulations mentioned above, glutamate-induced activation was enhanced by apamine (0.2 μmol·L^{-1}) and low Ca^{2+} containing aCSF, although only the former case was statistically significant ($n = 5$, $P < 0.05$ and $n = 6$, $P = 0.08$ respectively) (Table 1). This enhancement is likely to be due to blockade of slow after-hyperpolarizations, which shortens action potentials and thereby raises activation responses. Overall, these results indicate that the PAI induced by glutamate in the LC is mediated by a K^+ current resistant to conventional concentrations of TEA and not mediated by classical inwardly rectifying or Ca^{2+}-dependent channels.

Other Ca^{2+}-dependent intracellular signalling proteins (i.e. PKC and NO synthase) have also been shown to be involved in the modulation of glutamate receptors and synaptic responses (Bohme *et al*., 1991). However, neither 7-nitroindazole (30 μmol·L^{-1}, $n = 4$; and 100 μmol·L^{-1}, $n = 6$), an inhibitor of neuronal NO synthase, nor chelerythrine (20 μmol·L^{-1}, $n = 2$), a potent and selective PKC inhibitor, modified the magnitude of PAI (data not shown). This suggests that Ca^{2+} signalling mechanisms may not be involved in the PAI induced by glutamate.

Contribution of Na^+-dependent K^+ currents in the inhibitory effect of glutamate on LC neurons

Recently, K channels sensitive to high intracellular concentrations of Na^+ ions (K_{Na}) and rather resistant to TEA blockade (Yang *et al*., 2007) have been described in neurons of several brain nuclei (Bhattacharjee and Kaczmarek, 2005; Yang *et al*., 2007). These K_{Na} can be readily triggered by application of AMPA (Nanou and El Manira, 2007). Therefore, we used different manipulations affecting these channels (Yang *et al*., 2006; 2007) to explore whether they would mediate the inhibitory effect of glutamate. In three out of four neurons, perfusion with bithionol (1, 3 and 10 μmol·L^{-1}), an effective activator of K_{Na}, enhanced glutamate-induced PAI in a concentration-dependent manner (changes induced by bithionol: +14%, $n = 2$; +50%, $n = 2$; and +147%, $n = 3$, $P < 0.05$; respectively) (Table 1; Figure 6A). Interestingly, the early activation induced by glutamate was not modified significantly by bithionol (1, 3 and 10 μmol·L^{-1}) (changes induced by bithionol: –15%, $n = 2$; +1%, $n = 2$; and –24%,

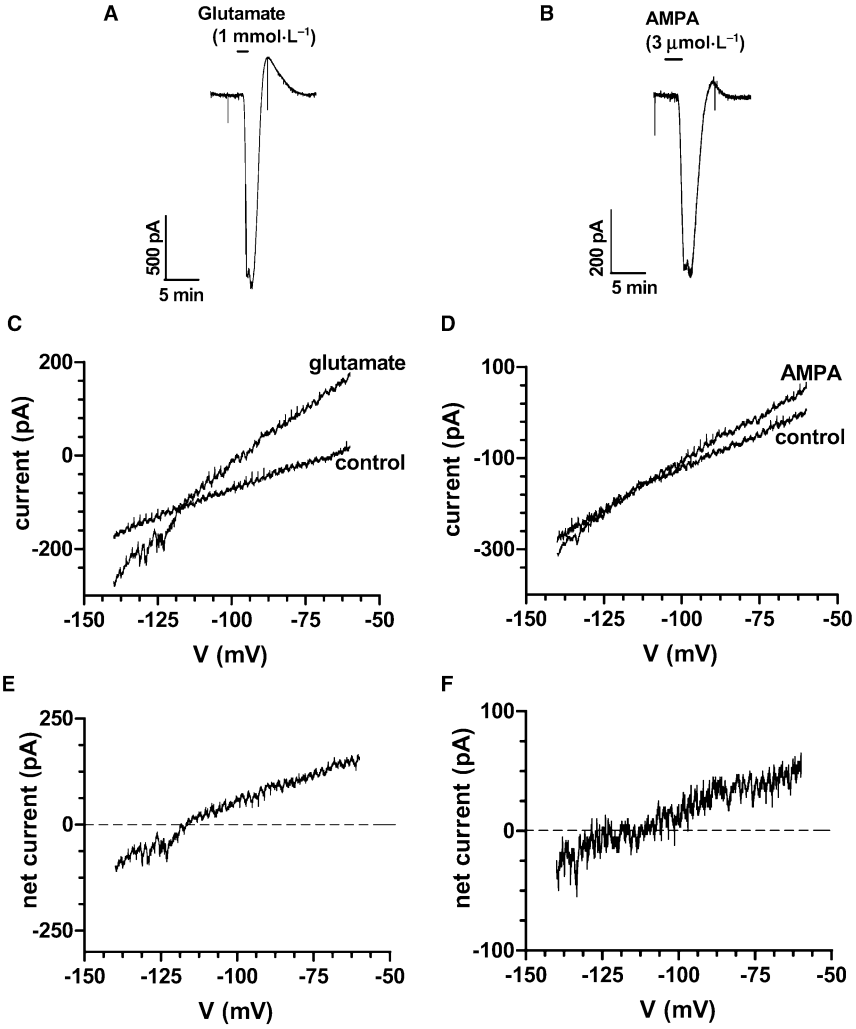

Figure 5 Effect of glutamate and AMPA on membrane currents of LC neurons. A, B. Representative samples of membrane currents induced by glutamate (1 mmol·L^{-1}) (A) and AMPA (3 µmol·L^{-1}) (B) in neurons voltage-clamped at −60 mV. Drugs were perfused for the duration shown by the bars. C–F. Representative samples of voltage-current relations recorded before drugs (control) and during the PAI induced by glutamate (C) or AMPA (D). The corresponding net currents were estimated (E, F) from the differences between the currents after drugs and the control. The reversal potential of net currents was −110 mV and −102 mV respectively.

$n = 3$; respectively) (Table 1; Figure 6A). There was a non-significant reduction in the spontaneous firing rate of LC neurons during bithionol (10 µmol·L^{-1}) perfusion (firing rate, basal: 0.47 ± 0.09 Hz; bithionol: 0.33 ± 0.03 Hz; $n = 3$). On the other hand, decreasing by a 80% the Na^+ concentration in the bathing aCSF (equiosmolarly replaced by choline) significantly blocked both activation and PAI induced by glutamate (Table 1; Figure 6B) and by AMPA (ratios: 0.39 ± 0.07, $n = 4$, $P < 0.01$; and 0.38 ± 0.14, $n = 4$, $P < 0.01$; respectively) (Figure 6B). No change in NMDA effect was found, however, after Na^+ replacement (ratio for activation: 1.12 ± 0.27, $n = 4$; the PAI was not observed) (Figure 6B). A lower reduction in the Na^+ concentration (up to 60%) of the aCSF did not modify glutamate-induced effects ($n = 7$) (Table 1), suggesting a precise regulation of these currents by intracellular Na^+ concentrations.

Activation of K_{Na} has been described to require large changes in intracellular Na^+ concentrations (Yang *et al.*, 2006; Nanou and El Manira, 2007), which would be reached only through AMPA receptors highly permeable to Na^+ ions. Therefore, we performed reverse transcription polymerase chain reaction (RT-PCR) experiments to explore the presence of the AMPA receptor subunits GluR1 (Ca^{2+}-permeable) and GluR2 (Ca^{2+}-impermeable) in the LC. These assays allowed us to detect a high level of mRNA for both AMPA receptor subunits GluR1 and GluR2 in the LC as well as in the cerebral cortex (which was used as a control region) (Figure 6C). The presence of GluR2 would render AMPA receptors Ca^{2+}-impermeable (Hara and Snyder, 2007) and thereby highly prone to Na^+ fluxes. Therefore, these data suggest that Na^+-dependent K channels may be responsible, at least in part, for the inhibitory effect of glutamate on LC neurons.

Discussion

There is evidence, obtained *in vivo,* that sensory stimuli evoke inhibitory responses in the LC, which are triggered by initial

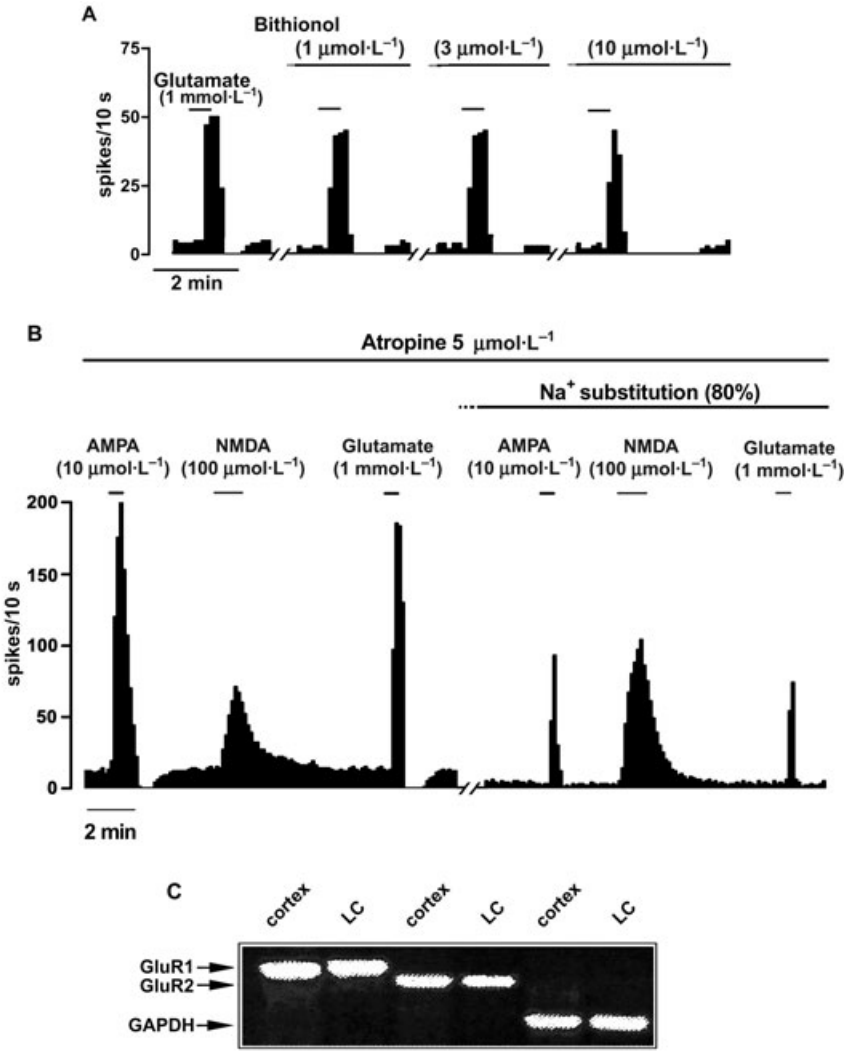

Figure 6 Contribution of Na^+-activated K channels in the inhibitory effect of glutamate on locus coeruleus neurons. A. Representative example of the firing rate recording of a neuron showing the effect of glutamate (1 mmol·L^{-1}, 30 s) before and after 10 min applications of increasing concentrations of bithionol (1–10 μmol·L^{-1}). Each vertical line represents the integrated firing rate (spikes per 10 s). Drugs were bath applied at the concentration and for the time indicated by the horizontal bars. Note that under both conditions (before and after bithionol) glutamate was able to induce a post-activation inhibition, but the duration of that inhibition was longer after bithionol, which expresses an enhanced inhibition. B. Representative example of the firing rate recording of a neuron showing the effect of AMPA (10 μmol·L^{-1}, 30 s), NMDA (100 μmol·L^{-1}, 60 s) and glutamate (1 mmol·L^{-1}, 30 s) before and after Na^+ substitution in the aCSF (80%) with choline for 10 min. C. PCR analysis of GluR1 and GluR2 expressed in the rat cerebral cortex and LC. mRNA expression for GAPDH was used as an internal control.

activations dependent on glutamate release (Ennis and Aston-Jones, 1986; 1988). The aim of this electrophysiological study was to directly investigate in brain slices whether glutamate mimics the activation/inhibition effect in the LC and the possible underlying mechanisms. Our results demonstrate that glutamate causes a biphasic response in most LC cells, with an initial activation of the firing activity followed by a late inhibition (PAI). An AMPA/kainate receptor antagonist attenuated glutamate-induced PAI and, in agreement, PAI was observed with AMPA and quisqualate (a mixed iGluR/mGluR agonist). Accordingly, in whole-cell patch-clamp experiments, glutamate and AMPA caused inward followed by late outward currents.

Glutamate, NMDA, AMPA and kainate induce strong excitation of LC neurons by a direct depolarization of postsynaptic neurons (Olpe *et al.*, 1989; Ennis *et al.*, 1992; Kogan and Aghajanian, 1995), which fits well with the presence of most cloned iGluR subunits in LC neurons (Sato *et al.*, 1993; Wisden and Seeburg, 1993; Petralia *et al.*, 1994; Watanabe *et al.*, 1994). mGluRs play a more relevant role at presynaptic level in the LC (Fotuhi *et al.*, 1993; Ohishi *et al.*, 1993; Dubé and Marshall, 1997). In our work, a short application of glutamate elicited a concentration-dependent activation of LC neurons, comparable to that found by other authors (Kogan and Aghajanian, 1995). Effective glutamate concentrations were similar to those published in the LC [2 mmol·L^{-1} focally applied *in vivo* (Tokuyama *et al.*, 2001); 10 mmol·L^{-1} locally applied in slices (Dubé and Marshall, 1997); 1 mmol·L^{-1} bath perfused in slices (Kogan and Aghajanian, 1995)], and not very different from the peak glutamate con-

centration (1.1 mmol·L^{-1}) measured at cultured synapses (Clements *et al.*, 1992). The potency rank order estimated from our concentration-effect curves was: AMPA > kainate > NMDA > glutamate, equivalent to that observed in earlier *in vitro* reports (Olpe *et al.*, 1989). An AMPA/kainate receptor antagonist (CNQX), but not a NMDA receptor blocker (D-AP5), reduced the activation induced by glutamate in the LC. Likewise, activation of LC cells by glutamatergic afferents *in vivo* seems to be mediated by AMPA/kainate receptors (Ennis and Aston-Jones, 1988), whereas LC cell activation by glutamate *in vitro* is partially blocked by selective AMPA receptor antagonists (Rasmussen *et al.*, 1996).

Regarding the inhibitory effect, 81% of the LC neurons in our study responded to glutamate with a late cessation of the firing activity after the activation. Similar biphasic inward-outward currents were recorded after glutamate application by whole-cell patch-clamp assays. *In vitro* and *in vivo* studies have shown that activation of LC cells by intracellular depolarizing pulses evokes a non-specific inhibition, which is reduced by Cd^{2+} and depends on the level of initial activation (Aghajanian and VanderMaelen, 1982; Andrade and Aghajanian, 1984). In our work, PAI was not blocked by Cd^{2+} and the phenomenon occurred regardless of the degree of previous activation. Thus, various drugs (e.g. CNQX, Cd^{2+}, TEA or apamine) only affected glutamate-induced activation, whereas bithionol only altered glutamate-induced PAI. More importantly, high concentrations of NMDA caused strong levels of activation but failed to induce PAI. Likewise, strong activation of LC cells without occurring inhibition can be elicited by other agonists (e.g. nicotinic acetylcholine receptor agonists) (Egan and North, 1986). Finally, an outward current was elicited by glutamate when the cell was clamped at −60 mV and thereby not firing. Therefore, the PAI we describe herein does not seem to be secondary to intrinsic spike-induced, Ca^{2+}-activated currents.

It has been described *in vivo* that non-selective glutamate receptor antagonists, but not NMDA receptor blockers, attenuate electrophysiological excitatory/inhibitory responses of LC cells to sensory stimuli (Ennis and Aston-Jones, 1988). Likewise, we have found in the LC *in vitro* that an AMPA/kainate receptor blocker (CNQX), but not a NMDA receptor (D-AP5) or an mGluR (RS-MCPG; Roberts, 1995; Dubé and Marshall, 1997) antagonist, attenuates glutamate-induced PAI. Accordingly, two AMPA/kainate receptor agonists (AMPA and the mixed AMPA/metabotropic glutamate receptor agonist quisqualate; Roberts, 1995) were able to induce PAI in a concentration-related manner. AMPA also caused a late outward conductance measured by whole-cell patch-clamping. Conversely, high concentrations of NMDA, kainate or tACPD (an mGluR agonist; Roberts, 1995; Dubé and Marshall, 1997) or various combinations of iGluR/mGluR agonists, failed to cause PAI. The failure of NMDA or tACPD to induce the PAI can not be attributed to the slower washout rates of these agonists compared with glutamate, AMPA or quisqualate (Collingridge *et al.*, 1983; Schneggenburger *et al.*, 1992; Wang and French, 1995). However, a slower recovery has been reported for kainate (Collingridge *et al.*, 1983; Schneggenburger *et al.*, 1992; Wang and French, 1995), and therefore we can not exclude that a late inhibition was masked by a prolonged activation. Taken together, our experiments suggest that AMPA/kainate receptors may mediate the glutamate-induced PAI.

Antidromic activation of LC neurons by electrical stimuli in the dorsal noradrenergic bundle *in vivo* causes a post-excitatory inhibition that is blocked by α_2-adrenoceptor antagonists and hence mediated by noradrenaline release (Aghajanian *et al.*, 1977; Ennis and Aston-Jones, 1986). In our study, two different α_2-adrenoceptor antagonists (RS79948 and idazoxan; Fernández-Pastor and Meana, 2002) were unable to change glutamate-induced PAI. Other receptors that have been well characterized to mediate inhibition of LC neurons (i.e. μ opioid, A_1 adenosinic or $GABA_{A/B}$ receptors) were also ruled out by selective receptor antagonists (Pepper and Henderson, 1980; Olpe *et al.*, 1988; Regenold and Illes, 1990). Finally, blocking the release of neurotransmitters with a Ca channel blocker (Cd^{2+}) or low Ca^{2+} containing aCSF failed to modify the extent of PAI. These results indicate that presynaptic release of inhibitory neurotransmitters may not be required in the glutamate-induced PAI *in vitro*. The finding that α_2-adrenoceptor antagonists attenuate sensory-evoked postexcitation inhibition *in vivo* (Cedarbaum and Aghajanian, 1978) suggests that, in the entire animal, sensory stimulation may activate extrinsic noradrenaline- or adrenaline-mediated inhibitory inputs in addition to the intrinsic mechanism of glutamate reported herein.

Given that a presynaptic mechanism does not seem to explain glutamate-induced PAI in the LC, we explored whether a somatodendritic ionic event was involved. Weakening the driving force of K^+ currents by raising the extracellular K^+ concentrations blunted glutamate-induced PAI. Likewise, in whole-cell experiments, the glutamate- and AMPA-induced outward currents reversed polarity close to the predicted reversal potential of K^+. However, conventional K^+ fluxes may not mediate glutamate-induced PAI, since it was not attenuated by the general K channel blocker TEA (Osmanovic and Shefner, 1990) or by blockade of inward-rectifier K channels (with Ba^{2+}), small- and large-conductance Ca^{2+}-activated K channels (with apamine and charybdotoxin respectively; and Cd^{2+} or low Ca^{2+} containing aCSF) or Na^+/K^+ exchanger (with ouabain). Finally, glutamate-induced PAI was not altered by PKC or neuronal NO synthase inhibitors (chelerythrine and 7-nitroindazole respectively), in contrast to other brain regions where glutamate-evoked hyperpolarization is modulated by Ca^{2+}-dependent inositol triphosphate signalling and NO synthesis (Bohme *et al.*, 1991; O'Dell *et al.*, 1991; Schuman and Madison, 1991; Fiorillo and Williams, 1998). These observations suggest that glutamate-induced PAI in the LC may be mediated by an intrinsic K^+ current different from classical Ca^{2+}-dependent or inward-rectifier K channels.

Recently, a novel family of TEA-resistant, Na^+-activated K^+ currents (K_{Na}) in brain neurons has been reported to contribute to the slow after-hyperpolarization following burst firing (Bhattacharjee and Kaczmarek, 2005; Yang *et al.*, 2007). Activation of K_{Na} requires large elevations of intracellular Na^+, such as those occurring after repetitive firing periods (Bhattacharjee and Kaczmarek, 2005; Yang *et al.*, 2006) or after application of AMPA (Nanou and El Manira, 2007). In our study, perfusion with bithionol, a K_{Na} activator (Yang *et al.*, 2006;

2007), potentiated glutamate-induced PAI in a concentration-dependent manner, whereas it did not change glutamate-induced activation. In agreement, Na^+ substitution (80%) in the aCSF markedly reduced the glutamate-induced PAI. However, 60% Na^+ replacement failed to modify glutamate effects, indicating a fine control of these currents by Na^+ concentrations. RT-PCR assays for AMPA receptor subunits found high mRNA levels for GluR2 in the LC, which should make AMPA receptors rather impermeable to Ca^{2+} (Hara and Snyder, 2007). Therefore, a higher probability of intense Na^+ fluxes through AMPA receptors in the LC could allow activation of putative Na^+-dependent K channels in these neurons. Future research should be conducted to confirm the hypothesis that K_{Na} channels are involved in the inhibitory effect of glutamate on LC neurons.

In conclusion, our study demonstrates that glutamate causes a biphasic response in the LC, including a strong PAI. Our data reveal that glutamate-induced PAI is a specific event, probably triggered by AMPA/kainate receptors. A postsynaptic intrinsic mechanism that depends on an atypical, Na^+-dependent K^+ current, rather than a presynaptic release of inhibitory neurotransmitters, could underlie glutamate-induced PAI. The physiological relevance of glutamate-induced effects is straightforward considering the integrative function played by the LC and glutamate in brain reactions (Aston-Jones and Cohen, 2005). In fact, it could be speculated that the mechanisms postulated herein *in vitro* could be further extrapolated to *in vivo* reactions to sensory stimuli.

Acknowledgements

This work was supported by grants from Ministerio de Ciencia y Tecnología (SAF2008-03612), Ministerio de Salud y Consumo (MSC-FIS) (RTA G03/005 and PI05/0513), Basque Government (PE04UN12), University of the Basque Country (1/UPV 0026.327-E-15924/2004 and GIU07/46) and Plan Nacional sobre Drogas (PND-MSC 2005). T.Z. was supported by a predoctoral fellowship from the Basque Government.

Conflict of interest

The authors state no conflict of interest.

References

Aghajanian GK, Vandermaelen CP (1982). a2-Adrenoceptor-mediated hyperpolarization of locus coeruleus neurons: intracellular studies in vivo. *Science* **215**: 1394–1396.

Aghajanian GK, Cedarbaum JM, Wang RY (1977). Evidence for norepinephrine-mediated collateral inhibition of locus coeruleus neurons. *Brain Res* **136**: 570–577.

Aghajanian GK, Vandermaelen CP, Andrade R (1983). Intracellular studies on the role of calcium in regulating the activity and reactivity of locus coeruleus neurons in vivo. *Brain Res* **273**: 237–243.

Alexander SPH, Mathie A, Peters JA (2008). Guide to Receptors and Channels (GRAC), 3rd edn. *Br J Pharmacol* **153** (Suppl. 2): S1–S209.

Andrade R, Aghajanian GK (1984). Locus coeruleus activity *in vitro*: intrinsic regulation by a calcium-dependent potassium conductance but not alpha 2-adrenoceptors. *J Neurosci* **4**: 161–170.

Aston-Jones G, Cohen JD (2005). An integrative theory of locus coeruleus-norepinephrine function: adaptive gain and the role and optimal performance. *Annu Rev Neurosci* **28**: 403–450.

Bailey CP, Couch D, Johnson E, Griffiths K, Kelly E, Henderson G (2003). μ-Opioid receptor desensitization in mature rat neurons: lack of interaction between DAMGO and morphine. *J Neurosci* **23**: 10515–10520.

Berridge CW, Waterhouse BD (2003). The locus coeruleus-noradrenergic system: modulation of behavioral state and state-dependent cognitive processes. *Brain Res Rev* **42**: 33–84.

Bhattacharjee A, Kaczmarek LK (2005). For K^+ channels, Na+ is the new Ca^{2+}. *Trends Neurosci* **28**: 422–428.

Bohme GA, Bon C, Stutzmann J, Doble A, Blanchard J (1991). Possible involvement of nitric oxide in long-term potentiation. *Eur J Pharmacol* **199**: 379–381.

Cedarbaum JM, Aghajanian GK (1976). Noradrenergic neurons of the locus coeruleus: inhibition by epinephrine and activation by the α-antagonist piperoxane. *Brain Res* **112**: 413–419.

Cedarbaum JM, Aghajanian GK (1978). Activation of locus coeruleus neurons by peripheral stimuli: modulation by a collateral inhibitory mechanism. *Life Sci* **23**: 1383–1392.

Chao J, Nestler EJ (2004). Molecular neurobiology of drug addiction. *Annu Rev Med* **55**: 113–132.

Chiang C, Aston-Jones G (1993). Response of locus coeruleus neurons to footshock stimulation is mediated by neurons in the rostral ventral medulla. *Neuroscience* **53**: 705–715.

Clements JD, Lester RA, Tong G, Jahr CE, Westbrook GL (1992). The time course of glutamate in the synaptic cleft. *Science* **258**: 1498–1501.

Collingridge GL, Kehl SJ, McLennan H (1983). Excitatory amino acids in synaptic transmission in the Schaefer collateral-commissural pathway of the rat hippocampus. *J Physiol* **334**: 33–46.

Dahlstrom A, Fuxe K (1965). Evidence for the existence of an outflow of noradrenaline nerve fibres in the ventral roots of the rat spinal cord. *Experientia* **21**: 409–410.

Dubé GR, Marshall KC (1997). Modulation of excitatory synaptic transmission in locus coeruleus by multiple presynaptic metabotropic glutamate receptors. *Neuroscience* **80**: 511–521.

Egan TM, North RA (1986). Actions of acetylcholine and nicotine on rat locus coeruleus neurons *in vitro*. *Neuroscience* **19**: 565–571.

Ennis M, Aston-Jones G (1986). Evidence for self- and neighbor-mediated post-activation inhibition of locus coeruleus neurons. *Brain Res* **374**: 299–305.

Ennis M, Aston-Jones G (1988). Activation of locus coeruleus from nucleus paragigantocellularis: new excitatory amino acid pathway in brain. *J Neurosci* **8**: 3644–3657.

Ennis M, Aston-Jones G, Shiekhattar R (1992). Activation of locus coeruleus neurons by nucleus paragigantocellularis or noxious sensory stimulation is mediated by intracoerulear excitatory amino acid neurotransmission. *Brain Res* **598**: 185–195.

Fernández-Pastor B, Meana JJ (2002). In vivo tonic modulation of the noradrenaline release in the rat cortex by locus coeruleus somatodendritic alpha(2)-adrenoceptors. *Eur J Pharmacol* **442**: 225–229.

Fiorillo CD, Williams JT (1998). Glutamate mediates an inhibitory postsynaptic potential in dopamine neurons. *Nature* **394**: 78–82.

Foote SL, Aston-Jones G, Bloom FE (1980). Impulse activity of locus coeruleus neurons in awake rats and monkeys is a function of sensory stimulation and arousal. *Proc Natl Acad Sci USA* **77**: 3033–3037.

Fotuhi M, Sharp AH, Glatt CE, Hwang PM, von Krosigk M, Snyder SH *et al*. (1993). Differential localization of phosphoinositide-linked metabotropic glutamate receptor (mGluR1) and the inositol 1,4,5-triphosphate receptor in rat brain. *J Neurosci* **13**: 2001–2012.

Hara MR, Snyder SH (2007). Cell signaling and neuronal death. *Ann Rev Pharmacol Toxicol* **47**: 117–141.

Kogan JH, Aghajanian GK (1995). Long-term glutamate desensitization in locus coeruleus neurons and its role in opiate withdrawal. *Brain Res* **689**: 111–121.

Masuko S, Nakajima Y, Nakajima S, Yamaguchi K (1986). Noradrenergic neurons from the locus coeruleus in dissociated cell culture: culture methods, morphology, and electrophysiology. *J Neurosci* **6**: 3229–3241.

Nanou E, El Manira A (2007). A postsynaptic negative feedback mediated by coupling between AMPA receptors and Na^+-activated K^+ channels in spinal cord neurones. *Eur J Neurosci* **25**: 445–450.

Nestler EJ, Aghajanian GK (1997). Molecular and cellular basis of addiction. *Science* **278**: 58–63.

O'Dell TJ, Hawkins RD, Kandel ER, Arancio O (1991). Tests of the roles of two diffusible substances in long-term potentiation: evidence for nitric oxide as a possible early retrograde messenger. *Proc Natl Acad Sci USA* **88**: 11285–11289.

Ohishi H, Shigemoto R, Nakanishi S, Mizuno N (1993). Distribution of the mRNA for a metabotropic glutamate receptor (mGluR3) in the rat brain: an in situ hybridization study. *J Comp Neurol* **335**: 252–266.

Olpe HR, Steinmann MW, Hall RG, Brugger F (1988). G_ABAA and GABAB receptors in locus coeruleus: effects of blockers. *Eur J Pharmacol* **149**: 183–185.

Olpe HR, Steinmann MW, Brugger F, Pozza MF (1989). Excitatory amino acid receptors in rat locus coeruleus. An extracellular *in vitro* study. *Naunyn-Schmiedebergs Arch Pharmacol* **339**: 312–314.

Osmanovic SS, Shefner SA (1990). Gamma-Aminobutyric acid responses in rat locus coeruleus neurones *in vitro*: a current-clamp and voltage-clamp study. *J Physiol* **421**: 151–170.

Pepper CM, Henderson G (1980). Opiates and opioid peptides hyperpolarize locus coeruleus neurons *in vitro*. *Science* **209**: 394–395.

Petralia RS, Yokotani N, Wenthold RJ (1994). Light and electron microscope distribution of the NMDA receptor subunit NMDAR1 in the rat nervous system using a selective anti-peptide antibody. *J Neurosci* **14**: 667–696.

Pineda J, Ruiz-Ortega JA, Martin-Ruiz R, Ugedo L (1996). Agmatine does not have activity at alpha 2-adrenoceptors which modulate the firing rate of locus coeruleus neurones: an electrophysiological study in rat. *Neurosci Lett* **219**: 103–106.

Rasmussen K, Kendrick WT, Kogan JH, Aghajanian GK (1996). A selective AMPA antagonist, LY293558, suppresses morphine withdrawal-induced activation of locus coeruleus neurons and behavioral signs of morphine withdrawal. *Neuropsychopharmacology* **15**: 497–505.

Regenold JT, Illes P (1990). Inhibitory adenosine A1-receptors on rat locus coeruleus neurones. An intracellular electrophysiological study. *Naunyn-Schmiedeberg Arch Pharmacol* **341**: 225–231.

Roberts PJ (1995). Pharmacological tools for the investigation of metabotropic glutamate receptors (mGluRs): phenylglycine derivatives and other selective antagonists-an update. *Neuropharmacology* **34**: 813–819.

Sato K, Kiyama H, Tohyama M (1993). The differential expression patterns of messenger RNAs encoding non-N-methyl-D-aspartate glutamate receptor subunits (GluR1-4) in the rat brain. *Neuroscience* **52**: 515–539.

Schneggenburger R, Lopez-Barneo J, Konnerth A (1992). Excitatory and inhibitory synaptic currents and receptors in rat medial septal neurones. *J Physiol* **445**: 261–276.

Schuman EM, Madison DV (1991). A requirement for the intercellular messenger nitric oxide in long-term potentiation. *Science* **254**: 1503–1506.

Svensson TH, Bunney BS, Aghajanian GK (1975). Inhibition of both noradrenergic and serotonergic neurons in brain by the alpha-adrenergic agonist clonidine. *Brain Res* **92**: 291–306.

Tokuyama S, Zhu H, Oh S, Ho IK, Yamamoto T (2001). Further evidence for a role of NMDA receptors in the locus coeruleus in the expression of withdrawal syndrome from opioids. *Neurochem Int* **39**: 103–109.

Wang T, French ED (1995). NMDA, Kainate, and AMPA depolarize nondopamine neurons in the rat ventral tegmentum. *Brain Res Bull* **36**: 39–43.

Watanabe M, Mishina M, Inoue Y (1994). Distinct spatiotemporal expressions of five NMDA receptor channel subunit mRNAs in the cerebellum. *J Comp Neurol* **343**: 513–519.

Wisden W, Seeburg PH (1993). A complex mosaic of high-affinity kainate receptors in rat brain. *J Neurosci* **13**: 3582–3598.

Yang B, Gribkoff VK, Pan J, Damagnez V, Dworetzky SI, Boissard CG, Bhattacharjee A *et al.* (2006). Pharmacological activation and inhibition of *Slack (Slo2.2*) channels. *Neuropharmacology* **51**: 896–906.

Yang B, Desai R, Kaczmarek LK (2007). Slack and Slick K_{Na} channels regulate the accuracy of timing of auditory neurons. *J Neurosci* **27**: 2617–2627.